

# Analysis of a PDE to model Dislocation Motion

Luca Bollini

## Contents

<b>1</b>	<b>Introduction</b>	<b>2</b>
1.1	Sketch . . . . .	2
1.2	Geometry . . . . .	2
1.3	Discovery . . . . .	3
1.4	Motion . . . . .	4
<b>2</b>	<b>Modelling</b>	<b>6</b>
2.1	Setup . . . . .	6
2.2	Force Balance . . . . .	7
2.3	Challenges . . . . .	11
2.4	Nondimensionalization . . . . .	12
2.5	The Non-linear Equation . . . . .	13

# 1 Introduction

## 1.1 Sketch

In February 2023, renowned strength sports athlete Vispy Kharadi broke the world record for most iron rods bent over the head in one minute, achieving an impressive total of 24. You can watch an overly dramatic video of this feat here: [Most Iron Bars Bent](#). While one might first wonder what would possess a person to take on such a challenge, or if bending metal rods over your head is medically advisable (it's not), as mathematicians, we ask a different question: "How do metals bend?". A physicist might quickly produce an answer such as: "Well, the man's head is exerting a shear stress force on the rod, causing defects in the crystalline structure of the metal, called *dislocations*, to move. This results in the atoms rearranging themselves into the shape of a bent iron rod.". We will go one step further. In this project, we formally introduce a model for the movement of a line dislocation, analysing the existence of solutions to the following linearised PDE. We then finish with a discussion about extending this model to include regions of different materials, simulating an alloy or a composite. Before we embark, let's give a summary of what dislocations are, and how they were discovered.

## 1.2 Geometry

Throughout this chapter, there will be numerous references to "Introduction to Dislocations" by Hull and Bacon [7], which can be regarded as the definitive source of background information regarding this topic. Their precise formulation of crystallographic defects' geometric structure and rich exploration of observational techniques are a fantastic way to immerse yourself in this theory.

*Dislocations* are the linear defects in crystalline structures responsible for plastic deformation. All crystalline materials can have these defects, but it is in metals that most of the interesting behaviour occurs; other materials such as coal and ceramics either have too few dislocations, or crack more easily than they are able to deform plastically. There are two types of dislocation: *edge* and *screw*. Let's outline how they look on the atomic level.

Imagine a simple cubic structure of atoms, as in figure (??), where we think of the vertical and horizontal lines as bonds between atoms, while the atoms themselves are placed at each intersection. Let's assume we may model the bonds as flexible springs between adjacent atoms, thus avoiding the complexity of how bonding works in real solids. What follows is a sequence of operations to describe how a dislocation can be formed from a

perfect crystal:

1. Break all the bonds intersecting the half-plane defined by  $ABCD$ .  $CD$  is the *leading-edge*, where our dislocation is to be positioned, and the half-plane extends upwards in the direction of  $\vec{CB}$ .
2. For an edge dislocation, insert a half-plane of atoms where the bonds have just been broken. This is shown in figure (??)<sup>1</sup>.

For a screw dislocation, shift all the atoms on one side of  $ABCD$  by one bond length in the direction  $\vec{AB}$ . This can result in one of two chiral structures depending on which direction the shift is in; a shift by  $+\vec{AB}$  is the mirror image of a shift by  $-\vec{AB}$ . The “left-handed” version is illustrated in figure (??).

Note that both types of dislocation distort the bonds close to the leading-edge  $CD$ , and that this distortion decreases with distance. This will be relevant in section 2.2 when discussing line tension.

Furthermore, we can see how these structures allow for the easy rearrangement of atomic bonds under shear. Figure (??) shows two layers of the cross section of a perfect crystal on the left, and an edge dislocation on the right. If we apply a shear force to the perfect crystal, we will need to break every bond along  $EF$  before shifting the top layer one to the left and reforming the bonds. Such an action requires immense force, much more than is observed in practice. In contrast, applying the same to the crystal with an edge dislocation is relatively easy. We can just break and reform bonds one at a time to “fill the gap” caused by the dislocation. This requires several orders of magnitude less force. In fact, this phenomenon is exactly how dislocations were discovered.

### 1.3 Discovery

Modern dislocation theory first appeared in the 1930s following calculations to determine the theoretical critical stress of materials. By *critical stress*, we mean the maximum stress a material can withstand before deforming plastically. As laid out by Hull and Bacon [7, § 1.4], this was done in 1926 by Frenkel, who showed the shearing force required to move one row of atoms across another is given by the equation

$$\tau = \frac{Gb}{2\pi a} \sin \frac{2\pi x}{b}$$

where  $b$  is the spacing of atoms in the direction of shear,  $a$  is the spacing between rows of atoms,  $x$  is the displacement of the two rows from the stable position, and  $G$  is the elastic modulus, or elastic shear stiffness, of

---

<sup>1</sup>(reference diagram style as being similar to [7, § 1.4])

the material. Figure (??) illustrates this setup. Realistic calculations for the maximum shearing force yield theoretical critical stresses around  $\tau_{th} \approx \frac{G}{30}$ . This is strikingly different from observational data, which indicates that critical stresses are generally between  $10^{-8}G$  and  $10^{-4}G$ .

The mystery behind such contrast was solved in 1934, when three scientists, Orowan, Talyor and Polyani, independently theorised the presence of dislocations and reasoned that they could account for the difference between prediction and experiment. Their work induced an explosion of research into dislocations throughout the 1940s and into the early 1950s, which is when the famous Peach-Koehler equation [8] was first presented. We will make use of this in section 2.2. It wasn't until 1956 that direct observation of dislocation movement was made by electron microscopy (figure (??)).

## 1.4 Motion

Central to dislocation motion is the concept of the *Burgers circuit* and *Burgers vector*. “A Burgers circuit in a crystal containing dislocations is an atom-to-atom path which forms a closed loop” [7, § 1.4]. Crucially, if the same path is made in a crystal containing no dislocation, and the path does not close, then the circuit must contain at least one dislocation. You can see this in figure (??), where (a) shows a Burgers circuit encapsulating an edge dislocation, while (b) shows the same path superimposed onto a dislocation-free crystal. The vector required to close the loop is labelled as the *Burgers vector*. Furthermore, we can see from figure (??) that the Burgers vector of any edge dislocation is perpendicular to its dislocation line (the line is going into the page). For screw dislocations, the Burgers vector is parallel to the dislocation line.

In this project, we shall be modelling the movement of an arbitrary dislocation (either edge or screw) under conservative motion, called *glide*. Dislocations capable of glide are called *glissile*, and the resulting process is known as *slip*; two planes of atoms slide over one another, while the only moving part is the dislocation itself. Think of this like using a squeegee to remove an air bubble trapped in a sticker. The dislocation is the air bubble and the squeegee is the shear force inducing slip. The sticker creeps forward as the air bubble moves, which you can imagine as the planes of atoms sliding over each other while the dislocation leads the way.

In figure (??), we can see that regions of crystal either side of the so-called *slip plane* remain undisturbed, and that the Burgers vector is depicted as being parallel to the direction of motion. This is because neighbouring atoms across the slip plane move relative to each other by precisely the Burgers vector. You can find many detailed diagrams of this in Hull and Bacon's book. It is for this reason that the Burgers vector is so important in dislocation motion.

Finally, we'll discuss slip planes in more depth. For edge dislocations,

note the Burgers vector and dislocation line are enough to uniquely specify the slip plane, while for screw dislocations this is not the case. We will always impose, however, that motion is confined to a single slip plane and further use that the Burgers vector lies in this plane.

We now aim to formally write down a model for the motion of a dislocation undergoing glide, then prove existence and uniqueness results for the derived equation.

## 2 Modelling

### 2.1 Setup

Let's first consider a static dislocation, figure (??). Curve  $\gamma$  represents the dislocation line in  $\mathbb{R}^3$ . The defect has fluctuations away from the  $x$ -axis entirely contained in the  $xy$ -plane, consistent with the observation of real dislocations in figure (??). We shall only consider the dislocation for  $0 \leq x \leq L$  with  $L$  finite, since real solids can only ever contain a dislocation of finite length. Moreover, we will assume control of  $L$ , making it as large as we wish while keeping the fluctuations of  $\gamma$  uniformly bounded. This will be a prominent feature in this model as we readily choose to send

$$\varepsilon = \frac{\lambda}{L} \rightarrow 0,$$

where  $\lambda > 0$  is the maximum deviation of  $\gamma$  away from the  $x$ -axis.

Another important aspect of this model will be our assumption that  $\gamma$  can be parametrised by  $\varphi(x) = (x, f(x), 0)^T$  for some  $f : [0, L] \rightarrow \mathbb{R}$ . We say that  $\gamma$  is of *graphical* form — the main novelty in this project. This is in contrast to other dislocation models such as the Frank-Read source (c.f. Hudson et al.), where geometric calculus overlooks the model's analysis; we will instead get to work in just one dimension.

Next, we prescribe *periodic boundary conditions* to  $\gamma$ . That is,  $\varphi(0) = \varphi(L)$  and  $\varphi'(0) = \varphi'(L)$ . For this reason, we'll shift to viewing the problem on the torus in chapter 3 (??), but only consider  $x \in (0, L)$  while deriving the model.

Additionally, notice how no assumption is being made about the type of dislocation, nor the Burgers vector. Both edge and screw dislocations exhibit the same behaviour when subjected to forcing, and hence will have no effect on our modelling assumptions.

*Remark 2.1.* It's worth noting that while it seems reasonable to assume  $\gamma$  is continuously differentiable, we do not make the same assumption about  $f$ . Later on, we'll see how our model makes sense even when  $f$  is defined almost everywhere, and this is in fact very much desired. We may want to simulate dislocations such as figure (??), where  $f'(x) \rightarrow \infty$  as  $x \rightarrow x_0$  and we make no attempt to define  $f$  at  $x_0$ . Any analysis we perform should be robust enough to take care of edge-cases like this.

Now let's introduce motion. We let  $\gamma(t)$  be a family of regular curves for  $t \in [0, T]$  which lie entirely in the  $xy$ -plane. In the language of section 1.4, the  $xy$ -plane is the *active slip plane*, where the motion of our dislocation will be described. We will hereafter project the problem onto this plane wherever possible. Again assuming graphical form, we parametrise the dislocation at time  $t$  by

$$\varphi(x, t) = (x, u(x, t), 0)^T \tag{1}$$

with  $u : [0, L] \times [0, T] \rightarrow \mathbb{R}$  differentiable in time. We will soon show how a non-linear PDE in  $u$  can be formed under the assumption of *Quasi-static evolution*, meaning forces acting on at any point must balance at all times. The forces in question are friction, line tension, and applied shear stress.

To summarise, here are the key features of this model, which are also illustrated in figure (??):

#### Key features

- The dislocation curves are assumed to have graphical form (1).
- Periodic boundary conditions hold at all times  $t$ :

$$u(0, t) = u(L, t) \text{ and } \partial_t u(0, t) = \partial_t u(L, t).$$

- We may choose  $L$  to be considerably larger than  $\lambda$ , where

$$\lambda = \sup_{[0, L]} |u(x, 0)|$$

is the initial maximum deviation of the dislocation from the  $x$ -axis, provided  $\int_0^L u(x, 0) dx = 0$ . We'll make use of this by sending  $\varepsilon = \frac{\lambda}{L}$  to 0.

- Motion is via Quasi-static evolution, balancing forces at all times.

## 2.2 Force Balance

To balance any forces and derive a PDE, we must first establish how we can write down each force in question: friction, line tension and applied stress. Friction is the simplest. For any object in motion, we can write down the elementary relation

$$\mathbf{f}_{\text{friction}} = -\mu \mathbf{v},$$

where  $\mathbf{v}$  is the velocity of the object, and  $\mu$  the coefficient of friction. This also applies to dislocations, however we must be precise;  $\mathbf{f}_{\text{friction}}$  is the *force per unit length* acting on the curve. Therefore, we should multiply by the length of curve in consideration to obtain the frictional force we use in the balance argument.

Next, let's look at line tension. After studying the geometry of dislocations, we noted how the bonds between atoms are distorted near the dislocation site, and that distortion decreases with distance. Anderson et al. [2, § 6.5] describe how this distortion can be interpreted as locally exerting a line tension force on the dislocation line<sup>2</sup>, which acts by “straightening the

<sup>2</sup>However, Anderson et al. also note that “the analogy is not exact, and the meaning of

curve” as if it were elastic. By letting  $E_0$  be the coefficient of dislocation stiffness<sup>3</sup>, the line tension force that point  $A$  exerts on a neighbouring point  $B$  is expressed as

$$\mathbf{f}_{\text{tension}} = E_0 \mathbf{t}.$$

Here,  $\mathbf{t}$  is the unit tangent vector to the curve at point  $A$ , directed away from point  $B$ .

Now for applied stress per unit length, we can use the Peach-Koehler force mentioned in section 1.3 [8]

$$\mathbf{f}_{\text{stress}} = (\boldsymbol{\sigma} \mathbf{b}) \times \mathbf{t},$$

where  $\boldsymbol{\sigma}$  is the external stress field,  $\mathbf{b}$  is the Burgers vector, and  $\mathbf{t}$  is the oriented unit tangent to the dislocation line. We’ll assume the stress field is uniform with components  $\sigma_{ij}$ . Stress fields inducing conservative motion are necessarily symmetric by conservation of angular momentum, so we are free to assume  $\sigma_{ij} = \sigma_{ji}$ . Let’s restate that we don’t make any assumption about the Burgers vector other than lying in the glide plane. The Burgers vector is therefore expressed as  $\mathbf{b} = (b_1, b_2, 0)^T$ .

To derive an explicit expression for  $\mathbf{f}_{\text{stress}}$ , we compute

$$\begin{aligned} \boldsymbol{\sigma} \mathbf{b} &= \begin{pmatrix} \sigma_{11}b_1 + \sigma_{12}b_2 \\ \sigma_{12}b_1 + \sigma_{22}b_2 \\ \sigma_{13}b_1 + \sigma_{23}b_2 \end{pmatrix} =: \begin{pmatrix} \alpha_1 \\ \alpha_2 \\ \alpha_3 \end{pmatrix}, \\ \mathbf{t} &= \frac{1}{\sqrt{1 + (\partial_x u)^2}} (1, \partial_x u, 0)^T \end{aligned}$$

and so

$$(\boldsymbol{\sigma} \mathbf{b}) \times \mathbf{t} = \frac{1}{\sqrt{1 + (\partial_x u)^2}} \begin{pmatrix} -\alpha_3 \partial_x u \\ \alpha_3 \\ \alpha_1 \partial_x u - \alpha_2 \end{pmatrix}.$$

Appealing to the discussion in section 1.4, we assume the dislocation cannot escape the glide plane, so only the projection of this force into the glide plane will have an effect on dislocation motion. We therefore conclude

$$\mathbf{f}_{\text{stress}} = \tilde{\sigma} \mathbf{n},$$

where we’ve rebranded  $\sigma_{13}b_1 + \sigma_{23}b_2$  as  $\tilde{\sigma}$ , and  $\mathbf{n}$  is the unit normal vector,

$$\mathbf{n} = \frac{1}{\sqrt{1 + (\partial_x u)^2}} (-\partial_x u, 1, 0)^T.$$

---

*a line tension for a dislocation is somewhat nebulous*”. Our use of line tension is merely a local approximation of a much more complex picture.

<sup>3</sup>Strictly speaking,  $E_0$  may depend on the type of dislocation and orientation of the unit tangent:  $E_0(\mathbf{b} \cdot \mathbf{t})$ . This would introduce further non-linearity to the model, but not severe enough to warrant diverting our attention.



For the rest of this subsection, we fix a  $t \in [0, T]$ , dropping the explicit  $t$  dependence, and aim to balance the forces acting on a small section of the dislocation curve  $\gamma(t)$ . Let's also momentarily assume  $u$  is as differentiable as required to justify the following computations.

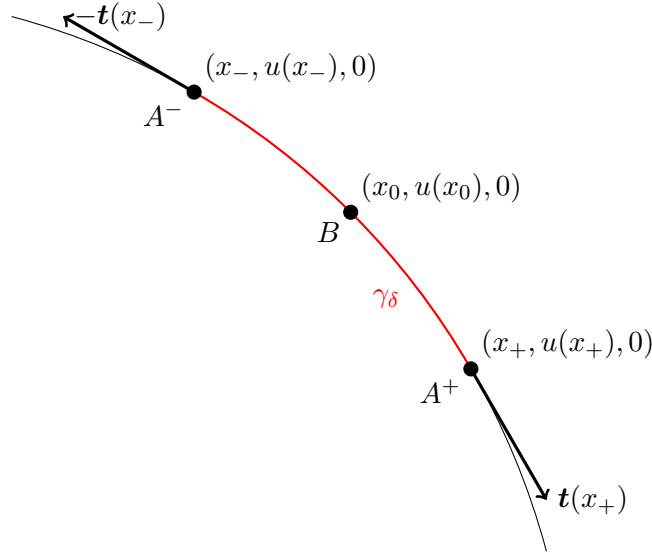


Figure 1: A small section of curve  $\gamma(t)$

Zooming in, as in figure 1, let  $\gamma_\delta$  be the section of curve between  $x_- = x_0 - \frac{\delta}{2}$  and  $x_+ = x_0 + \frac{\delta}{2}$ , for some  $x_0 \in (0, L)$  and small  $\delta > 0$ . We label points on the curve

$$\begin{aligned} B &= (x_0, u(x_0), 0)^T, \\ A^- &= (x_-, u(x_-), 0)^T, \\ A^+ &= (x_+, u(x_+), 0)^T \end{aligned}$$

and note that the length of  $\gamma_\delta$  is linearly approximated by

$$|\gamma_\delta| \approx \sqrt{\delta^2 + (u(x_+) - u(x_-))^2}.$$

This becomes a reasonable estimate when we send  $\delta$  to 0. In particular,

$$\frac{|\gamma_\delta|}{\delta} \rightarrow \sqrt{1 + (\partial_x u(x_0))^2} \quad \text{as } \delta \rightarrow 0. \quad (2)$$

As laid out above, we can easily see that the forces acting on  $B$  are

$$\begin{aligned} \mathbf{f}_{\text{tension}} &= E_0 \mathbf{t}(x_+) - E_0 \mathbf{t}(x_-), \\ \mathbf{f}_{\text{friction}} &= -|\gamma_\delta| \mu \mathbf{v}(x_0), \\ \mathbf{f}_{\text{stress}} &= |\gamma_\delta| \tilde{\sigma} \mathbf{n}(x_0), \end{aligned}$$

where the total line tension force is the sum of the forces acted on  $B$  by  $A^-$  and  $A^+$ . Therefore, we can conclude from our assumption of Quasi-static evolution

$$E_0 \mathbf{t}(x_+) - E_0 \mathbf{t}(x_-) + |\gamma_\delta| (-\mu \mathbf{v}(x_0) + \tilde{\sigma} \mathbf{n}(x_0)) = 0. \quad (3)$$

Dividing through by  $\delta$  and taking the dot product with  $\mathbf{n}(x_0)$ , we find

$$\frac{E_0 \mathbf{t}(x_+) - E_0 \mathbf{t}(x_-)}{\delta} \cdot \mathbf{n}(x_0) + \frac{|\gamma_\delta|}{\delta} (-\mu \mathbf{v}(x_0) \cdot \mathbf{n}(x_0) + \tilde{\sigma}) = 0.$$

If we take  $\delta \rightarrow 0$ , we can see from the definitions of  $x_-$  and  $x_+$  that

$$\frac{E_0 \mathbf{t}(x_+) - E_0 \mathbf{t}(x_-)}{\delta} \rightarrow E_0 \mathbf{t}'(x_0)$$

and so together with the limit (2),

$$E_0 \frac{\mathbf{t}'(x_0) \cdot \mathbf{n}(x_0)}{\sqrt{1 + (\partial_x u(x_0))^2}} - \mu \mathbf{v}(x_0) \cdot \mathbf{n}(x_0) + \tilde{\sigma} = 0. \quad (4)$$

Now referring back to the parametrisation (1), it is straightforward to compute

$$\mathbf{t}'(x) = \left( \partial_x \left( \frac{1}{\sqrt{1 + (\partial_x u)^2}} \right), \partial_x \left( \frac{\partial_x u}{\sqrt{1 + (\partial_x u)^2}} \right), 0 \right)^T \quad (5a)$$

$$\mathbf{n}(x) = \frac{1}{\sqrt{1 + (\partial_x u)^2}} (-\partial_x u, 1, 0)^T \quad (5b)$$

$$\mathbf{t}'(x) \cdot \mathbf{n}(x) = \sqrt{1 + (\partial_x u)^2} \partial_x \left( \frac{\partial_x u}{\sqrt{1 + (\partial_x u)^2}} \right), \quad (5c)$$

while in order to compute  $\mathbf{v}(x)$  we must think carefully about how points on the dislocation move. If, in equation (3), we instead take the dot product with  $\mathbf{t}(x_0)$  and let  $\delta \rightarrow 0$ , we observe (since both  $\mathbf{t}'$  and  $\mathbf{n}$  are orthogonal to  $\mathbf{t}$ )

$$-\mu \mathbf{v}(x_0) \cdot \mathbf{t}(x_0) = 0.$$

Together with the fact that the dislocation's motion is confined to the glide plane, we deduce that  $\mathbf{v}(x_0)$  is in the normal direction,  $\mathbf{n}(x_0)$ . Hence, the velocity vector is

$$\mathbf{v}(x_0) = (\partial_t \varphi(x_0) \cdot \mathbf{n}(x_0)) \mathbf{n}(x_0) = \frac{\partial_t u(x_0)}{\sqrt{1 + (\partial_x u(x_0))^2}} \mathbf{n}(x_0). \quad (6)$$

Finally, putting equations (4), (5) and (6) together we have derived the PDE

$$\mu \frac{\partial_t u}{\sqrt{1 + (\partial_x u)^2}} - E_0 \partial_x \left( \frac{\partial_x u}{\sqrt{1 + (\partial_x u)^2}} \right) = \tilde{\sigma}. \quad (7)$$

## 2.3 Challenges

At this point, we must make a few observations pertaining to the difficulty of tackling this equation. First of all, this is clearly a non-linear PDE. Especially so, since the bulk of non-linearity appears in the highest order derivative. However, as we shall see, this alone will not deter us from our endeavour. The primary challenge posed by equation (7) is the  $\sqrt{1 + (\partial_x u)^2}$  factor dividing the  $\partial_t u$  term. Multiplying through, we obtain

$$\mu \partial_t u - E_0 \sqrt{1 + (\partial_x u)^2} \partial_x \left( \frac{\partial_x u}{\sqrt{1 + (\partial_x u)^2}} \right) = \tilde{\sigma} \sqrt{1 + (\partial_x u)^2}.$$

Two challenges now emerge:

1. We see that the problematic factor is now affixed to the forcing term  $\tilde{\sigma}$ , so the equation is *advection-diffusion*, rather than pure diffusion. Whilst this may not appear like a trivial increase in complexity at first, it actually won't put up too much resistance against general quasi-linear PDE theory.
2. The more concerning issue is that we now see equation (7) is not of *divergence form* (more on this terminology later). This is a significant problem, as theory for non-divergence form PDEs is considerably less approachable than the theory for divergence form PDEs.

This second challenge prompts us to reconsider jumping straight into tackling such a problem head-on. Instead, we will first make a rather egregious simplification. By ignoring the  $\sqrt{1 + (\partial_x u)^2}$  factor dividing the  $\partial_t u$  term in equation (7), we have a (still non-linear) divergence form parabolic PDE which is much more approachable with functional analytic existence theory.

Contrary to first impressions, this simplification is not entirely dim-witted. With the right Nondimensionalization, it's possible to reason that each  $\sqrt{1 + (\partial_x u)^2}$  factor in equation (7) approaches 1 as some small parameter  $\varepsilon \rightarrow 0$ . As such, understanding this simplified case may lead us to explore the right concepts for understanding the full problem. Therefore, for at least the next two chapters of this project, we will instead work towards proving theoretical results for the following equation:

$$\mu \partial_t u - E_0 \partial_x \left( \frac{\partial_x u}{\sqrt{1 + (\partial_x u)^2}} \right) = \tilde{\sigma}. \quad (8)$$

Once we have a good grasp of how solutions to this PDE behave (provided they exist), we shall briefly discuss how one might extend the theory to the full equation (7).

## 2.4 Nondimensionalization

This subsection consists of three steps which reduce equation (8) to its simplest form:

1. Adding a correction term to  $u$  that removes constant forcing.
2. Nondimensionalization; using characteristic length scales of vertical fluctuations  $\lambda$ , and horizontal length  $L$  to reframe the problem with dimensionless quantities.
3. Redefining constants to write the equation in its simplest form.

Step one is to replace the function  $u$  with some  $U$  that corrects for the forcing term  $\tilde{\sigma}$  on the right hand side of (8). This is equivalent to changing coordinate frame into one that moves at a constant speed of  $\frac{\tilde{\sigma}}{\mu}t$  in the  $y$ -direction, thus following the dislocation as it propagates. This is achieved by defining

$$U(x, t) = u(x, t) - \frac{\tilde{\sigma}}{\mu}t,$$

which transforms (8) into

$$\mu \partial_t U - E_0 \partial_x \left( \frac{\partial_x U}{\sqrt{1 + (\partial_x U)^2}} \right) = 0.$$

The advantage of this formulation is that we impose a sort of “zero boundary values” simply by doing nothing; the integral  $\int_0^L U(x, t) dx$  will forever remain small if it starts at 0.

For the second step, we can define new dimensionless quantities  $\tilde{x}$  and  $\tilde{u}$  by

$$L\tilde{x} = x, \quad \lambda\tilde{u}(\tilde{x}, t) = U(x, t),$$

where  $\lambda = \sup_{[0, L]} |U(x, 0)|$  is the initial maximum deviation of the dislocation from the  $x$ -axis. A basic computation reveals

$$\mu\lambda\partial_t\tilde{u} - \frac{E_0\lambda}{L^2}\partial_{\tilde{x}} \left( \frac{\partial_{\tilde{x}}\tilde{u}}{\sqrt{1 + \left(\frac{\lambda}{L}\partial_{\tilde{x}}\tilde{u}\right)^2}} \right) = 0.$$

We complete step three by letting  $\varepsilon = \frac{\lambda}{L}$  and  $\kappa = \frac{E_0}{\mu L^2}$ . Dropping the tilde, this boils down to

$$\partial_t u - \kappa \partial_x \left( \frac{\partial_x u}{\sqrt{1 + (\varepsilon \partial_x u)^2}} \right) = 0. \tag{9}$$

## 2.5 The Non-linear Equation

We are now ready to formulate the problem we will be analysing for the rest of this project. Briefly note that the previous subsection has normalised the equation so that  $u : [0, 1] \times [0, T] \rightarrow \mathbb{R}$  and  $|u(x, 0)| \leq 1$  for every  $x \in [0, 1]$ . As discussed in section 2.1, we intend to assign periodic boundary conditions

$$u(0, t) = u(1, t), \quad \partial_t u(0, t) = \partial_t u(1, t) \quad (10)$$

to the model. An easy way to implement this is to redefine the problem on the one-dimensional torus,  $\mathbb{T} = \mathbb{R}/\mathbb{Z}$ . This way, if a solution to equation (9) is continuously differentiable on  $\mathbb{T}$ , it necessarily satisfies periodic boundary conditions (10) when viewed as a function on  $[0, 1]$ .

It is also worth pointing out that equation (9) looks strikingly similar to the heat equation:

$$\partial_t u - \kappa \partial_{xx} u = 0. \quad (11)$$

In fact, we should intuitively expect this to be the case. With the forcing removed, dislocation motion reduces to a form of *curve-shortening flow*, where sharp corners in the initial data are instantly made smooth — exactly as described by the heat equation. On closer inspection, setting  $\varepsilon = 0$  in equation (9) exactly recovers the heat equation, and it might be reasonable to expect solutions of (9) (provided they exist) to converge to solutions of the heat equation in some appropriate function space as  $\varepsilon \rightarrow 0$ . This will now be the main focus of the project.

The aims of the project are formally laid out in the following:

### The $\varepsilon$ -Problem

Define the  $\varepsilon$ -initial value problem

$$\begin{cases} \partial_t u^\varepsilon - \kappa \partial_x \left( \frac{\partial_x u^\varepsilon}{\sqrt{1 + (\varepsilon \partial_x u^\varepsilon)^2}} \right) = 0 & \text{in } \mathbb{T} \times (0, T] \\ u^\varepsilon = u_0^\varepsilon & \text{on } \mathbb{T} \times \{0\} \end{cases} \quad (\star)$$

where  $u_0^\varepsilon : \mathbb{T} \rightarrow \mathbb{R}$  is a given function with  $|u_0^\varepsilon| \leq 1$ , and  $u^\varepsilon : \mathbb{T} \times [0, T] \rightarrow \mathbb{R}$  is the unknown.

### Project aims

- Establish functional analytic results which demonstrate existence theory for uniformly parabolic PDEs.
- Show a unique solution to  $(\star)$  exists in an appropriate function space.
- Show solutions to  $(\star)$  converge to solutions of the heat equation (11) in an appropriate function space as  $\varepsilon \rightarrow 0$ .

Some citations: [5], [1], [6], [2], [7], [8], [4], [3].

## References

- [1] Aluminum in Space: Pushing the Limits of Aerospace Technology, 2024. URL <https://elkamehr.com/en/aluminum-in-space-pushing-the-limits-of-aerospace-technology/>. Accessed on 27th January 2025.
- [2] P. M. Anderson, J. P. Hirth, and J. Lothe. *Theory of dislocations*. Cambridge University Press, 2017.
- [3] Á. Bényi and T. Oh. The sobolev inequality on the torus revisited. *Publicationes Mathematicae Debrecen*, 83(3):359, 2013.
- [4] J. Colliander, M. Keel, G. Staffilani, H. Takaoka, and T. Tao. Sharp Global Well-Posedness for KdV and Modified KdV on  $\mathbf{R}$  and  $\mathbf{T}$ . *Journal of the American Mathematical Society*, 16(3):705–749, 2003.
- [5] L. C. Evans. *Partial differential equations*, volume 19. American Mathematical Society, 2 edition, 2022.
- [6] T. Hudson, F. Rindler, and J. Rydell. A quantitative model for the frank-read dislocation source based on pinned mean curvature flow. 2024. <https://arxiv.org/abs/2409.20294>.
- [7] D. Hull and D. J. Bacon. *Introduction to dislocations*, volume 37. 5 edition, 2011.
- [8] M. Peach and J. Koehler. The forces exerted on dislocations and the stress fields produced by them. *Physical Review*, 80(3):436, 1950.